Silicon Epitaxial Growth Accelerated by Parallel Langmuir Processes Using SiH_2Cl_2 and SiH_3CH_3 Gases

Ayami Yamada[1], Mitsuko Muroi[1], Toru Watanabe[1], Ayumi Saito[1], Ayumi Sakurai[1] and Hitoshi Habuka[1]

[1]Department of Chemistry Applications and Life Science, Yokohama National University

79-5 Tokiwadai Hodogaya, Yokohama 240-8501, Japan

e-mail: habuka-hitoshi-ng@ynu.ac.jp, Phone: +81-45-339-3998

The silicon epitaxial growth behaviour was studied as an application of the parallel-Langmuir process using SiH_2Cl_2 gas and SiH_3CH_3 gas. The SiH_3CH_3 gas was used for *in situ* producing the SiH_x gas by thermal decomposition in the reactor. With the increasing gas concentration of SiH_3CH_3, several results were obtained, such as (*i*) the silicon epitaxial growth rate increased exceeding the value saturated using the SiH_2Cl_2, (*ii*) the gas phase concentrations of the chlorosilanes at the exhaust decreased, (iii) the byproduct deposition at the exhaust decreased, and (iv) the gas phase concentration of HCl at the exhaust decreased. As a conclusion, the SiH_x helped consuming the SiH_2Cl_2 gas for producing a silicon epitaxial film with reducing the byproduct deposition. Additionally, the SiH_x might produce SiH_2Cl_2 in the gas phase by the reaction with the HCl gas.

Key words: Silicon epitaxial growth, parallel Langmuir processes, dichlorosilane, silicon hydrides

1. Introduction

For producing various electronic devices [1-3], silicon epitaxial films are prepared using trichlorosilane ($SiHCl_3$), dichlorosilane (SiH_2Cl_2), silane (SiH_4) and disilane (Si_2H_6) gases, in ambient hydrogen (H_2). For satisfying the expanding demands for technologies including the information, communication and power control, the silicon epitaxial growth process should have a high productivity. For this purpose, the epitaxial growth rate is one of the key issues.

Generally, the epitaxial growth rate can be increased by the increasing precursor supply. However, the silicon epitaxial growth rate in a chlorosilane-hydrogen system undergoes a saturation following the Eley-Rideal model [4, 5], when the surface is fully covered with the intermediate species at the sufficiently high chlorosilane concentrations. The issue for improving the epitaxial growth productivity is an additional process for exceeding such a saturation.

For this purpose, silicon hydride, SiH_x, was found to help overcome the growth rate saturation in the $SiHCl_3$-H_2 system, as reported in previous studies [6-8]. The mechanism was explained by the Langmuir processes, which were multiple and parallel at the surface. For expanding the application of this concept, the SiH_2Cl_2 gas [1, 9-11] should be studied as to whether it showed a behavior similar to the $SiHCl_3$ gas, because it was also a major precursor for the silicon epitaxial growth. Although the combination of SiH_2Cl_2 and SiH_4 was mainly evaluated by the plasma enhanced chemical vapour deposition (PECVD) [12-16], the thermal CVD process has been scarce [17-20].

The additional scientific advantage of SiH_2Cl_2 is fewer chlorine atoms which might experimentally clarify the chemical reaction of HCl with SiH_x for producing chlorosilanes in the gas phase.

In this study, the behavior of the silicon epitaxial growth rate in the SiH_2Cl_2-SiH_x-H_2 system was studied in detail for developing the silicon epitaxial process having a high productivity by applying the parallel-Langmuir process [6-8]. Additionally, the gas phase chemical reactions of HCl with SiH_x were experimentally evaluated.

2. Rate theory

Accounting for the parallel processes consisting of multiple precursors in various fields [17-24], the parallel-Langmuir process for the silicon epitaxial growth in a SiH_2Cl_2-SiH_x-H_2 system is assumed, as shown in Fig. 1, similar to that in the $SiHCl_3$-SiH_x-H_2 system [6-8]. In order to focus on the rate process governing the growth rate, the surface reactions and their reaction rates are assumed based on the following equations.

(A) Silicon epitaxial film production by SiH_2Cl_2 [1, 9]:

$$\mathrm{SiH_2Cl_2} \rightarrow * \mathrm{SiCl_2} + \mathrm{H_2}, \tag{1A}$$

$$V_{Ad} = k_{Ad}(1-\theta)[\mathrm{SiH_2Cl_2}]. \tag{1B}$$

$$* \mathrm{SiCl_2} + \mathrm{H_2} \rightarrow * \mathrm{Si} + 2\mathrm{HCl}, \tag{2A}$$

$$V_{r,1} = k_{r,1}\theta[\mathrm{H_2}]. \tag{2B}$$

$$* \mathrm{SiCl_2} + \mathrm{SiH}_x \rightarrow 2 * \mathrm{Si} + 2\mathrm{HCl} + \big((x-2)/2\big)\mathrm{H_2}. \tag{3A}$$

$$V_{r,2} = 2k_{r,2}\theta[\mathrm{SiH_x}]. \quad (3B)$$

"*" indicates the surface chemical species. θ is the surface coverage by *$SiCl_2$.

(B) Silicon epitaxial film production by SiH_x [1]:

$$\mathrm{SiH}_x \rightarrow * \mathrm{Si} + (x/2)\mathrm{H}_2 . \quad (4A)$$

$$V_{\mathrm{D}} = k_{\mathrm{D}}(1-\theta)[\mathrm{SiH_x}]. \quad (4B)$$

(C) The desorption of $SiCl_2$ from the surface [25, 26] :

$$* \mathrm{SiCl}_2 \rightarrow \mathrm{SiCl}_2. \quad (5A)$$

$$V_{\mathrm{ds}} = k_{\mathrm{ds}}\theta. \quad (5B)$$

Based on the Eley-Rideal model of the SiH_2Cl_2-H_2 system [1, 9], the silicon epitaxial growth is described by the following equation.

$$V_{\mathrm{G}} = \frac{k_{\mathrm{Ad}}k_{\mathrm{r,\,1}}[\mathrm{H_2}][\mathrm{SiH_2Cl_2}]}{k_{\mathrm{r,\,1}}[\mathrm{H_2}]+k_{\mathrm{Ad}}[\mathrm{SiH_2Cl_2}]}. \quad (6)$$

When the $k_{\mathrm{Ad}}[\mathrm{SiH_2Cl_2}]$ is significantly greater than $k_{\mathrm{r,\,1}}[\mathrm{H_2}]$, for increasing the growth rate by means of the high precursor concentration, the silicon epitaxial growth rate depends only on the H_2 gas concentration.

$$V_{\mathrm{G}} \cong k_{\mathrm{r,\,1}}[\mathrm{H_2}]. \quad (7)$$

Because the H_2 gas concentration is limited to that determined by the ambient pressure, equation (7) shows the upper limit, that is, it undergoes saturation.

Using equations (1A) – (5A), the θ value and the silicon film formation rate, V_G, were obtained taking into account the mass balance of the *$SiCl_2$.

$$\theta = \frac{k_{\mathrm{Ad}}[\mathrm{SiH_2Cl_2}]}{\left(k_{\mathrm{Ad}}[\mathrm{SiH_2Cl_2}]+k_{\mathrm{r,\,1}}[\mathrm{H_2}]+2k_{\mathrm{r,\,2}}[\mathrm{SiH_x}]+k_{\mathrm{ds}}\right)} \tag{8}$$

$$V_G = V_{r,1} + V_{r,2} + V_D = \frac{\left(k_{\mathrm{r,\,1}}[\mathrm{H_2}]+2k_{\mathrm{r,\,2}}[\mathrm{SiH_x}]\right)\left(k_{\mathrm{Ad}}[\mathrm{SiH_2Cl_2}]+k_{\mathrm{D}}[\mathrm{SiH_x}]\right)+k_{\mathrm{ds}}k_{\mathrm{D}}[\mathrm{SiH_x}]}{\left(k_{\mathrm{Ad}}[\mathrm{SiH_2Cl_2}]+k_{\mathrm{r,\,1}}[\mathrm{H_2}]+2k_{\mathrm{r,\,2}}[\mathrm{SiH_x}]+k_{\mathrm{ds}}\right)} \tag{9}$$

When $k_{\mathrm{Ad}}[\mathrm{SiH_2Cl_2}]$ is significantly greater than $k_{\mathrm{r,\,1}}[\mathrm{H_2}]$, $2k_{\mathrm{r,\,2}}[\mathrm{SiH}_x]$, k_{ds} and $k_{\mathrm{D}}[\mathrm{SiH}_x]$, the silicon epitaxial growth rate simply depends on the gas concentrations of H_2 and SiH_x, as equation (10).

$$V_G \cong k_{\mathrm{r,\,1}}[\mathrm{H_2}] + 2k_{\mathrm{r,\,2}}[\mathrm{SiH_x}] \tag{10}$$

As predicted by this equation, the silicon epitaxial growth rate in this system does not saturate, even when the SiH_2Cl_2 concentration is significantly high.

3. Experimental procedure

The silicon epitaxial film was formed using the reactor shown in Fig. 2. The (100) silicon wafer placed in the chamber was heated by halogen lamps. The chemical reaction was performed under the cold wall thermal condition. The SiH_3CH_3 gas and the SiH_2Cl_2 gas (Tri Chemical Laboratories, Inc., Yamanashi, Japan) were introduced with the H_2 gas (99.9999%, Sumitomo Seika Chemicals Co., Ltd., Tokyo Japan) from the inlet at atmospheric pressure for 20 min. For safety reasons, this study used SiH_3CH_3 gas instead of SiH_4 gas. The SiH_3CH_3 gas is supplied by vaporization from its liquid contained in a cylinder. It is very often used for producing silicon carbide thin films [27-30]. The SiH_3CH_3 gas is safely and thermally decomposed to produce SiH_x with CH_x in the gas phase [27]. The SiH_x produced from the SiH_3CH_3 was assumed to have the same effect as that the SiH_4 had. The H_2 flow rate was fixed at 1.05 slm. The SiH_3CH_3 flow rate was 0 – 15 sccm, while the SiH_2Cl_2 flow rate was 5 - 20 sccm. The wafer temperature was measured using a R-type thermocouple in an ambient nitrogen at various voltages loaded to halogen lamps, prior to the deposition. The wafer was heated at the halogen lamp voltage which could heat the wafer to 600 ^{o}C in nitrogen ambient. Such the low temperature was chosen for suppressing the unnecessary gas phase reactions.

This reactor did not have a susceptor for supporting the wafer. Additionally, a parasitic deposition on the chamber wall did not occur in this study. Thus, the depletion of any precursors did not occur before arriving at the wafer surface.

A part of the exhaust gas was fed to the quadrupole mass (QMS) analyzer (PrismaPlus QMG220, Pfeiffer Vacuum, Germany). The exhaust flange attached at the end of the chamber had a connecting port to the quartz crystal microbalance (QCM) sensor (25MHz, detection limit:

0.5 ng cm^{-2} Hz^{-1}, Halloran Electronics, Tokyo Japan). This sensor has a sufficient sensitivity and repeatability to detect any small weight change [25] less than that of the silicon monolayer (60 ng cm^{-2}). The frequency of the QCM sensor was monitored and recorded by a computer. The temperature of the exhaust flange was maintained lower than 40 ^{o}C during the silicon deposition process.

The epitaxial film thickness was measured by the micrometer and by the weight change of the substrate. The carbon incorporation from CH_x into the silicon epitaxial film was less than the detection limit of the X-ray photoelectron spectrometer (Quantera SXM, ULVAC-PHI Corp., Tokyo, Japan). In our previous study [6] performed in $SiHCl_3$-SiH_x-H_2 system, the secondary ion mass spectrometry (SIMS) showed that the carbon concentration was lower than the detection limit. Thus, the carbon incorporation was assumed to have no influence on the growth rate, similar to the previous study [6].

4. Results and discussion

4.1 Silicon epitaxial growth rate

Figures 3 shows the measurement of the silicon epitaxial growth rate obtained in the SiH_2Cl_2-H_2 system. Prior to this study, the epitaxial growth rate only by the SiH_x was determined to be significantly lower than that by the SiH_2Cl_2. As shown in Fig. 3, while the epitaxial growth rate by the SiH_2Cl_2 increased with the increasing SiH_2Cl_2 gas concentration, it saturated at 0.2 μm/min, which was the same rate as that saturated at 850 ^{o}C using the $SiHCl_3$-H_2 system in our previous study [6, 8]. The saturation behavior is explained by that predicted by equation (7).

Figure 4 shows the silicon epitaxial growth rate in the SiH_2Cl_2-SiH_x-H_2 system. With the increasing SiH_x flow rate, the silicon epitaxial growth rate in this system increased from 0.2 to 0.5 μm/min at the SiH_2Cl_2 gas concentrations of 10, 15 and 20 sccm, in a region where the silicon epitaxial growth rate saturated as shown in Fig. 3. This behavior was the same at the SiH_2Cl_2 gas concentrations of 10, 15 and 20 sccm. Thus, the silicon epitaxial growth rate was increased by the SiH_3CH_3 gas concentration, while it was not by the SiH_2Cl_2 gas concentration.

The scattering of the growth rate in Fig. 4 might be due to the reproducibility of wafer temperature which sensitively influenced the growth rate at the temperatures in the reaction limited region.

The tentative value of the rate constant obtained using the SiH_3CH_3 gas concentration at the inlet was 6×10^{-4} m s^{-1}, although the correct value should be determined taking into account the transport phenomena in the entire reactor [4, 5 and 8]. For evaluating the epitaxial film quality, various measurements, such as SIMS, photo-luminescence (PL) and lifetime measurement, are necessary.

Overall, this behavior was the same as that for the $SiHCl_3$-SiH_x-H_2 system. Thus, the parallel-Langmuir process was possible for SiH_2Cl_2 in addition to $SiHCl_3$.

4.2 Gas phase species

Figures 5 shows the mass spectra of the gas phase species contained in the exhaust gas during the silicon epitaxial growth measured by the QMS. When the epitaxial growth was performed using SiH_2Cl_2 and SiH_3CH_3 in ambient hydrogen, the $SiCl_2^+$ group near 98 amu was

assigned to the SiH_2Cl_2 and the $SiCl_2$. The $SiCl_2$ gas was caused by the thermal decomposition of SiH_2Cl_2 and the desorption from the silicon surface based on equation (5A) [25, 26]. The peaks near 63 amu was assigned to the fragments of SiH_2Cl_2 and $SiCl_2$. These were clearly observed with the byproduct of the HCl^+ group near 36 amu. Because the partial pressure of the $SiCl_3^+$ group was significantly low, the $SiHCl_3$ production by the gas phase reaction was negligible.

The SiH_3CH_3 was observed as the $SiH_yCH_z^+$ group in the mass region from 40 to 46 amu. The partial pressure peaks in the mass region between 28 and 32 indicate the SiH_x thermally decomposed in the gas phase and the fragment of SiH_3CH_3 occurred in the mass analyzer. The small peaks between 12 – 16 amu and that between 16 – 18 amu were assigned to CH_x and H_2O, respectively.

Figure 5 clearly showed that there were no peaks of $SiHCl_2CH_3$ (mass 115) and SiH_2ClCH_3 (mass 80). This indicated that the gas phase temperature in the cold wall thermal condition was sufficiently low to suppress the gas phase reaction between HCl and SiH_3CH_3 [27].

The epitaxial growth rate increase in Fig. 4 should be achieved by the effective consumption of SiH_2Cl_2. Figure 6 shows the partial pressures of $SiCl^+$, $SiCl_2^+$ and $SiCl_3^+$. With the increasing SiH_3CH_3 gas concentration, the partial pressure of the three chlorosilanes in the gas phase were shown to decrease. The summation of the normalized partial pressures were about 0.3 at the SiH_3CH_3 gas concentration of 0%. It decreased to less than 0.2 at the SiH_3CH_3 gas concentration of 1%. Thus, the SiH_3CH_3 addition was considered to enhance the SiH_2Cl_2 consumption.

Because the $SiCl_2^+$ group contains the gas phase species of $SiCl_2$, its decrease is expected to indicate the decrease in the $SiCl_2$ gas concentration in the reactor. This assumption was verified by the QCM. Figure 7 shows the deposition behavior of the byproduct which was $(SiCl_2)_n$ formed from the $SiCl_2$ gas in the gas phase [25]. Although the plots show significant scatter, the highest values at the various SiH_3CH_3 concentrations showed that the byproduct deposition decreased with the increasing SiH_3CH_3 concentration.

Next, the HCl gas concentration was evaluated. As indicated in Fig. 5, the HCl gas did not react with the SiH_3CH_3 gas, which could be stable because of the sufficiently low gas phase temperature. However, when the unstable intermediate species, such as the SiH_x, coexisted in the gas phase, it was expected to react with the HCl gas to cause various species, such as SiH_2Cl_2. Figure 8 shows the partial pressure of the HCl^+ group, normalized by that of the H_2^+ group. While the normalized partial pressure of HCl^+ was about 0.008 at the SiH_3CH_3 gas concentration of 0 %, it gradually decreased with the increasing SiH_3CH_3 gas concentration. At the SiH_3CH_3 gas concentration of 1 %, the normalized partial pressure of HCl^+ was about 0.004.

4.3 SiH_2Cl_2 production in gas phase

For evaluating the behavior of the HCl concentration in the gas phase, two chemical reactions to form the SiH_2Cl_2 were assumed, as shown in Fig. 9.

The first one is the SiH_2Cl_2 production from $SiCl_2$ and H_2.

$$SiCl_2 + H_2 \rightarrow SiH_2Cl_2 \qquad (11A)$$

$$V_{\mathrm{DCS1}}=k_{\mathrm{DCS1}}\ [\mathrm{SiCl_2}][\mathrm{H_2}] \tag{11B}$$

Equation (11A) is the reverse reaction of equation (1A) in the gas phase. The SiH_2Cl_2 is expected to have a reversible reaction with $SiCl_2$ and H_2 [10, 11]. However, the occurrence of equation (11A) cannot be verified by the QMS in this study, because the mass analyzer cannot accurately distinguish the $SiCl_2$ gas from the SiH_2Cl_2 gas and its fragments.

The second one is the SiH_2Cl_2 formation from SiH_x and HCl.

$$\mathrm{SiCl_x}+2\mathrm{HCl} \rightarrow \mathrm{SiH_2Cl_2} + \frac{x-2}{2}\ \mathrm{H_2} \tag{12A}$$

$$V_{\mathrm{DCS2}}=k_{\mathrm{DCS2}}\ [\mathrm{SiH_x}][\mathrm{HCl}]^n \tag{12B}$$

Equation (12B) was assumed to be the *n*-th order reaction. In the steady state and in the gas phase near the hot substrate surface, the summation of the HCl gas production rate by equations (2B) and (3B) was assumed to be the same as the HCl gas consumption rate by equation (12B). Additionally, equation (8) was taken into account to obtain the HCl gas concentration.

$$V_{\mathrm{r,\,1}} + \frac{1}{2}V_{\mathrm{r,\,2}}=V_{\mathrm{DCS2}} \tag{13}$$

$$k_{\mathrm{r,\,1}}\theta\ [\mathrm{H_2}]+ k_{\mathrm{r,\,2}}\theta\ [\mathrm{SiH_x}]=k_{\mathrm{DCS2}}[\mathrm{SiH_x}][\mathrm{HCl}]^n \tag{14}$$

$$[\mathrm{HCl}]^n = \left(\frac{k_{\mathrm{r,\,1}}\ [\mathrm{H_2}]}{k_{\mathrm{DCS2}}[\mathrm{SiH_x}]} + \frac{k_{\mathrm{r,\,2}}}{k_{\mathrm{DCS2}}}\right)\frac{k_{\mathrm{Ad}}[\mathrm{SiH_2Cl_2}]}{k_{\mathrm{Ad}}[\mathrm{SiH_2Cl_2}]+k_{\mathrm{r,\,1}}\ [\mathrm{H_2}]+2k_{\mathrm{r,\,2}}[\mathrm{SiH_x}]+k_{\mathrm{ds}}} \tag{15}$$

Based on equation (15), the HCl gas concentration decreases with the increasing SiH_x gas concentration. The SiH_x gas produced from the SiH_3CH_3 gas was expected to react with the HCl gas to cause the SiH_2Cl_2 gas. Equation (15) qualitatively agreed with the trend shown in Fig. 8. Equation (12A) was considered to compensate the decrease in the SiH_2Cl_2 concentration due to the consumption by the silicon epitaxial film formation.

This study focused on the reaction design. The further studies using wide conditions of the precursor concentration, the wafer temperature and the pressure should be performed. Additionally, the physical concepts, such as nucleation, phase change and super saturation, contained in the rate equation and the rate constant, should be extracted and clarified by any studies of the molecular dynamics, the quantum theory and the other methods.

6. Conclusions

The parallel-Langmuir process was evaluated for the silicon epitaxial growth in the SiH_2Cl_2-SiH_x-H_2 system. At a sufficiently high gas concentration of SiH_2Cl_2, while the silicon epitaxial growth rate saturated following the Eley-Rideal model, it exceeded and increased to a higher value with the increasing SiH_3CH_3 gas concentration. Simultaneously, at the exhaust, the chlorosilane gas concentration, the $(*SiCl_2)_n$ deposition rate and the HCl gas concentration decreased. Based on these results, the SiH_x gas was shown to have various roles, such as the acceleration of the $*SiCl_2$ decomposition at the surface and the SiH_2Cl_2 gas production in the gas phase. The parallel-Langmuir process was concluded to be possible for the silicon epitaxial

growth in the SiH_2Cl_2-SiH_x-H_2 system in order to improve the productivity of the silicon epitaxial film.

Acknowledgements

A part of this study was supported by JSPS KAKENHI grant No. 17K06904.

References

[1] D. Crippa, D. L. Rode, and M. Masi, Silicon Epitaxy, Academic Press (San Diego, USA, 2001).

[2] http://www.semi.org/jp/jp/MarketInfo/SiliconShipmentStatistics

[3] US Patent 4,364,073 "Power MOSFET with an anode region"

[4] H. Habuka, T. Nagoya, M. Mayusumi, M. Katayama, M. Shimada and K. Okuyama, Model on transport phenomena and epitaxial growth of silicon thin film in $SiHCl_3$-H_2 system under atmospheric pressure, J. Crystal Growth, 169, 61-72 (1996).

[5] H. Habuka, J. Suzuki, Y. Takai, H. Hirata and S. Mitani, Silicon epitaxial growth process using trichlorosilane gas in a single-wafer high-speed substrate rotation reactor, J. Crystal Growth, 327, 1-5 (2011).

[6] A. Saito, A. Sakurai and H. Habuka, Increase in silicon film deposition rate in a $SiHCl_3$-SiH_x-H_2 system, J. Crystal Growth, 468, 204-207 (2017).

[7] A. Sakurai, A. Saito and H. Habuka, Surface and gas phase reactions induced in a trichlorosilane-SiH_x system for silicon film deposition, Surf. Coat. Technol., 272, 273–277 (2015).

[8] T. Watanabe, A. Yamada, A. Saito, A. Sakurai and H. Habuka, Parallel Langmuir Processes for Silicon Epitaxial Growth in a $SiHCl_3$-SiH_x-H_2 System, Materials Science in Semiconductor Processing, 72, 134-138 (2017).

[9] Y. Ohshita, A. Ishitani and T. Takada, Surface reaction mechanism of $SiCl_2$ with carrier gas H_2 in silicon vapor phase epitaxial growth, J. Crystal Growth, 108 (3-4), 499-507 (1991).

[10] K. L. Knutson, R. W. Carr, W. H. Liu, S. and A. Campbell, A kinetics and transport model of dichlorosilane chemical vapor deposition, J. Crystal Growth, 140 (1–2), 191-204 (1994)

[11] F. Langlais, F. Hottier, and R. Cadoret, Chemical vapour deposition of silicon under reduced pressure in a hot-wall reactor: Equilibrium and kinetics, J. Crystal Growth, 56(3) 659-672 (1982).

[12] L. Guo, Y. Toyoshima, M. Kondo, and A. Matsuda, Low-temperature growth of crystalline silicon on a chlorine-terminated surface, Appl. Phys. Lett. 75, 3515 (1999).

[13] I. S. Osborne, N. Hata, and A. Matsuda, Stable hydrogenated amorphous silicon films deposited from silane and dichlorosilane by radio frequency plasma chemical vapor deposition, Appl. Phys. Lett. 66, 965 (1995).

[14] R. Platz and S. Wagner, Plasma-enhanced chemical vapor deposition of intrinsic microcrystalline silicon from chlorine-containing source gas, J. Vacuum Sci. Technol. A, 16, 3218 (1998).

[15] M. Nakata and S. Wagner, Fast growth of hydrogenated amorphous silicon from dichlorosilane, Appl. Phys. Lett. 65, 1940 (1994).

[16] H. Rauscher, F. Behrendt, and R. J. Behm, Fabrication of surface nanostructures by scanning tunneling microscope induced decomposition of SiH_4 and SiH_2Cl_2, J. Vacuum Sci. Technol. B, 15, 1373 (1997).

[17] A. M. Waite, N. S. Lloyd, K. Osman, W. Zhang, T. Ernst, H. Achard, Y. Wang, S. Deleonibus, P. L. F. Hemment, D. M. Bagnall, A. G. R. Evans, and P. Ashburn, Raised

source/drains for 50 nm MOSFETs using a silane/dichlorosilane mixture for selective epitaxy, Solid-State Electronics, 49 (4), 529-534 (2005).

[18] J. M. Hartmann, V. Benevent, M. Veillerot and A. Halimaoui, Potentialities of disilane for the low temperature epitaxy of intrinsic and boron-doped SiGe, Thin Solid Films, 557, 19-26 (2014).

[19] J. M. Hartmann, V. Benevent, J. F. Damlencourt and T. Billon, A benchmarking of silane, disilane and dichlorosilane for the low temperature growth of group IV layers, Thin Solid Films, 520 (8), 3185-3189 (2012).

[20] J. M. Hartmann, Impact of Si precursor mixing on the low temperature growth kinetics of Si and SiGe, The first joint conference of International SiGe Technology and Device Meeting (ISTDM) and International Conference on Silicon Epitaxy and Heterostructures (ICSI), Abstract page 117-118, (May 27-31, 2018, Potsdam, Germany).

[21] W. K. Burton, N. Cabrera and F. C. Frank, “The growth of crystals and the equilibrium structure of their surfaces”, Phil. Trans. Royal Soc., A243, 299-358 (1951).

[22] G. Sears, Influence of Adsorbed Films on Crystal Growth Kinetics, J. Chem. Phys. 25, 154 (1956).

[23] S.A. Kukushkin, A.V. Osipov, New phase formation on solid surfaces and thin film condensation, Progress in Surface Science, 151 (1), 1-107 (1996).

[24] S.A. Kukushkin, A.V. Osipov, Thin-film condensation processes, Physics-Uspekhi, 41(10), 983-1014 (1998).

[25] H. Habuka, A. Sakurai and A. Saito, By-product formation in a trichlorosilane-hydrogen system for silicon film deposition, ECS J. Solid State Sci. Technol., 4(2), P16-P19 (2015).

[26] P. A. Coon, P. Gupta, M. L. Wise, and S. M. George, Adsorption and desorption kinetics for SiH_2Cl_2 on Si(111) 7×7, J. Vacuum Sci. Technol. A, 10, 324 (1992).

[27] H. Habuka, M. Watanabe, Y. Miura, M. Nishida, T. Sekiguchi, Polycrystalline silicon carbide film deposition using monomethylsilane and hydrogen chloride gases, J. Crystal Growth, 300, 374-381 (2007).

[28] H. Nakazawa, M. Suemitsu, Dissociative adsorption of monomethylsilane on Si (100) as revealed by comparative temperature-programmed desorption studies on H/, C_2H_2/, and MMS/Si (100), Appl. Surf. Sci. 162–163, 139-145 (2000).

[29] K. Yasui, K. Asada, T. Maeda, T. Akahane, Growth of high quality silicon carbide films on Si by triode plasma CVD using monomethylsilane, Appl. Surf. Sci. 175–176, 495-498 (2001).

[30] T. Kaneko, N. Miyakawa, H. Yamazaki, Y. Iikawa, Growth kinetics in plasma CVD of a-SiC films from monomethylsilane revealed by in situ spectroscopy, J. Crystal Growth 237–239, 1260-1263 (2002).

Figure captions

Figure 1. Parallel-Langmuir process in a SiH_2Cl_2-SiH_x-H_2 system.

Figure 2 Horizontal cold wall reactor for silicon epitaxial growth used in this study.

Figure 3 Silicon epitaxial growth rate by SiH_2Cl_2 gas.

Figure 4 Silicon epitaxial growth rate by SiH_2Cl_2 and SiH_x gases.

Figure 5 Mass spectra of chemical species contained in the exhaust gas of the SiH_2Cl_2-SiH_x-H_2 system.

Figure 6 Partial pressures of $SiCl^+$, $SiCl_2^+$ and $SiCl_3^+$ groups.

Figure 7 Byproduct $(SiCl_2)_n$ deposition on QCM at various SiH_3CH_3 gas concentrations at the inlet.

Figure 8 HCl partial pressure at various SiH_3CH_3 concentrations.

Figure 9 Recycling between SiH_x, HCl, H_2 and SiH_2Cl_2 in the gas phase.

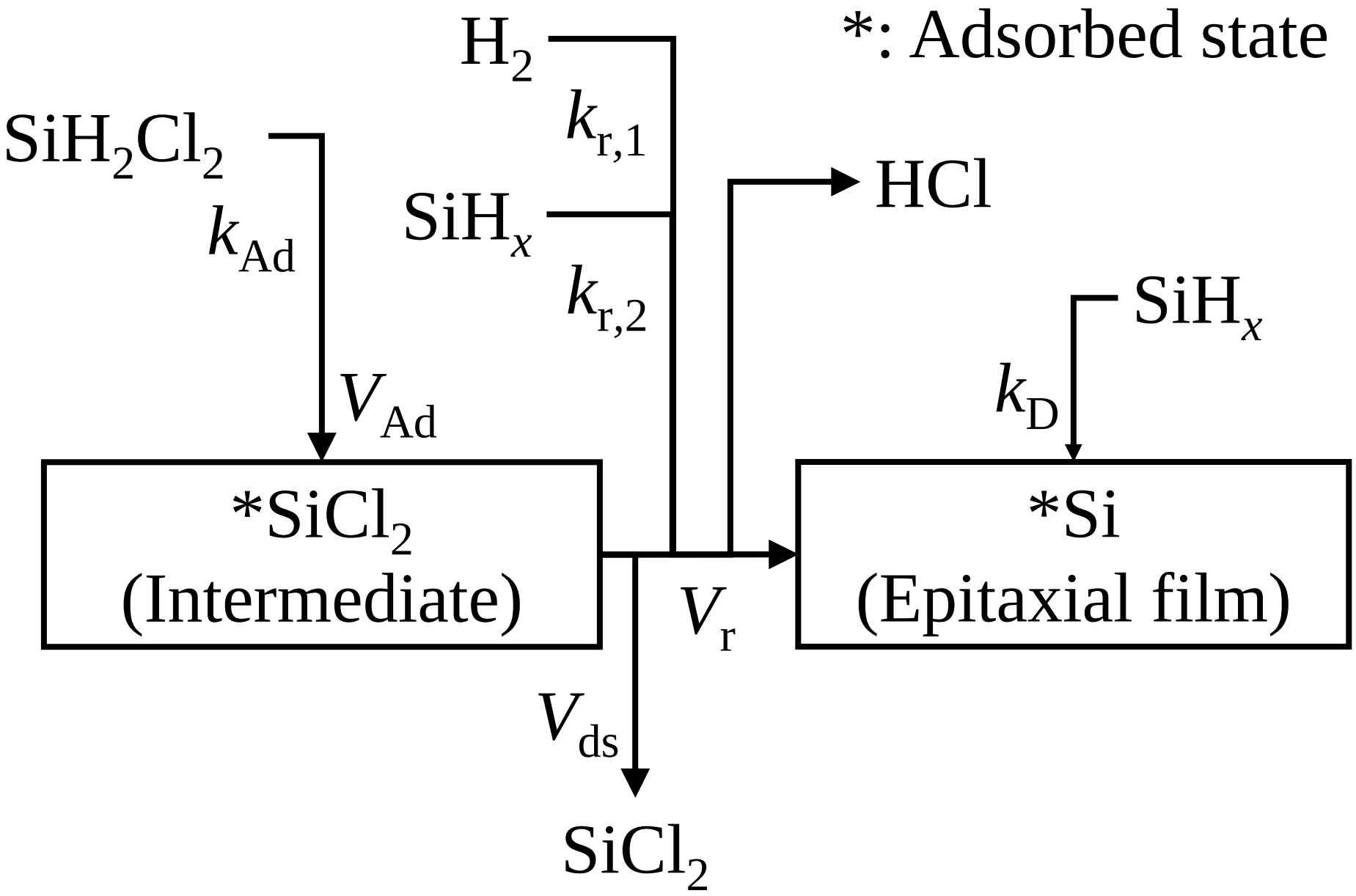
*: Adsorbed state
H2
kr,1
SiH2Cl2
kAd
SiHx
kr,2
HCl
SiHx
kD
VAd
*SiCl2
(Intermediate)
Vr
*Si
(Epitaxial film)
Vds
SiCl2

Fig. 1

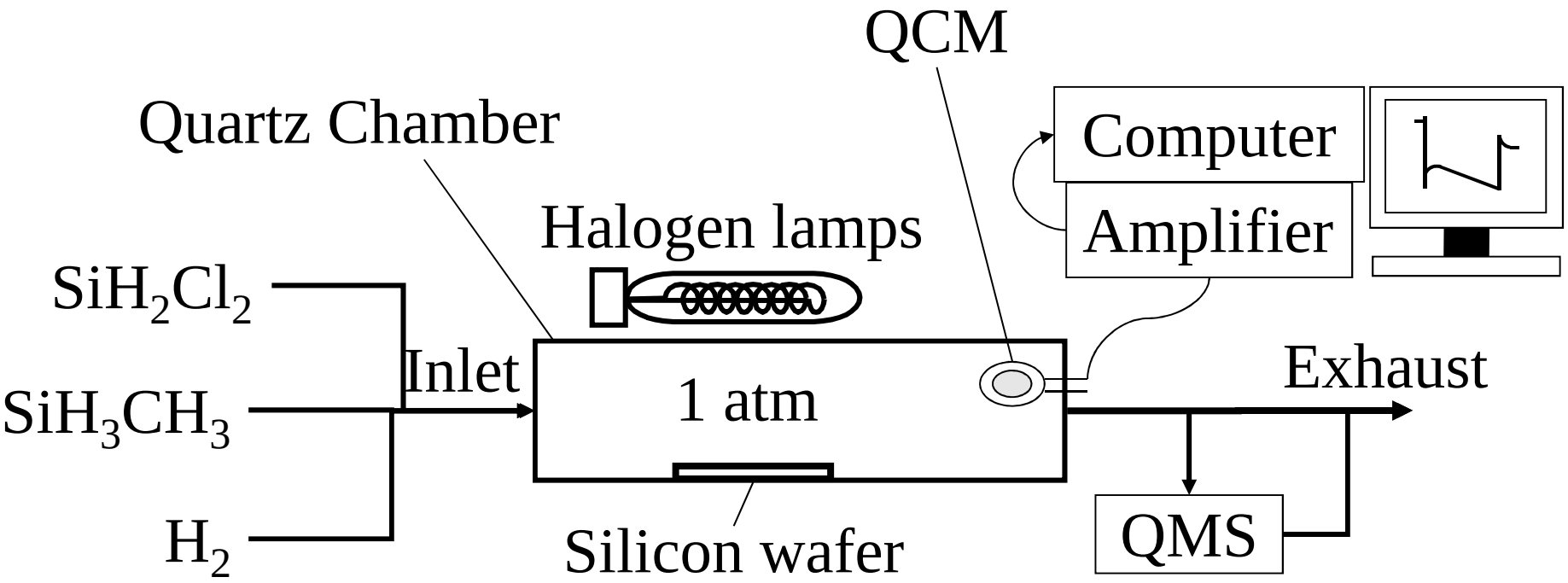
QCM
Quartz Chamber
Computer
Amplifier
Halogen lamps
SiH_2Cl_2
Inlet
1 atm
Exhaust
SiH_3CH_3
H_2
Silicon wafer
QMS

Fig. 2

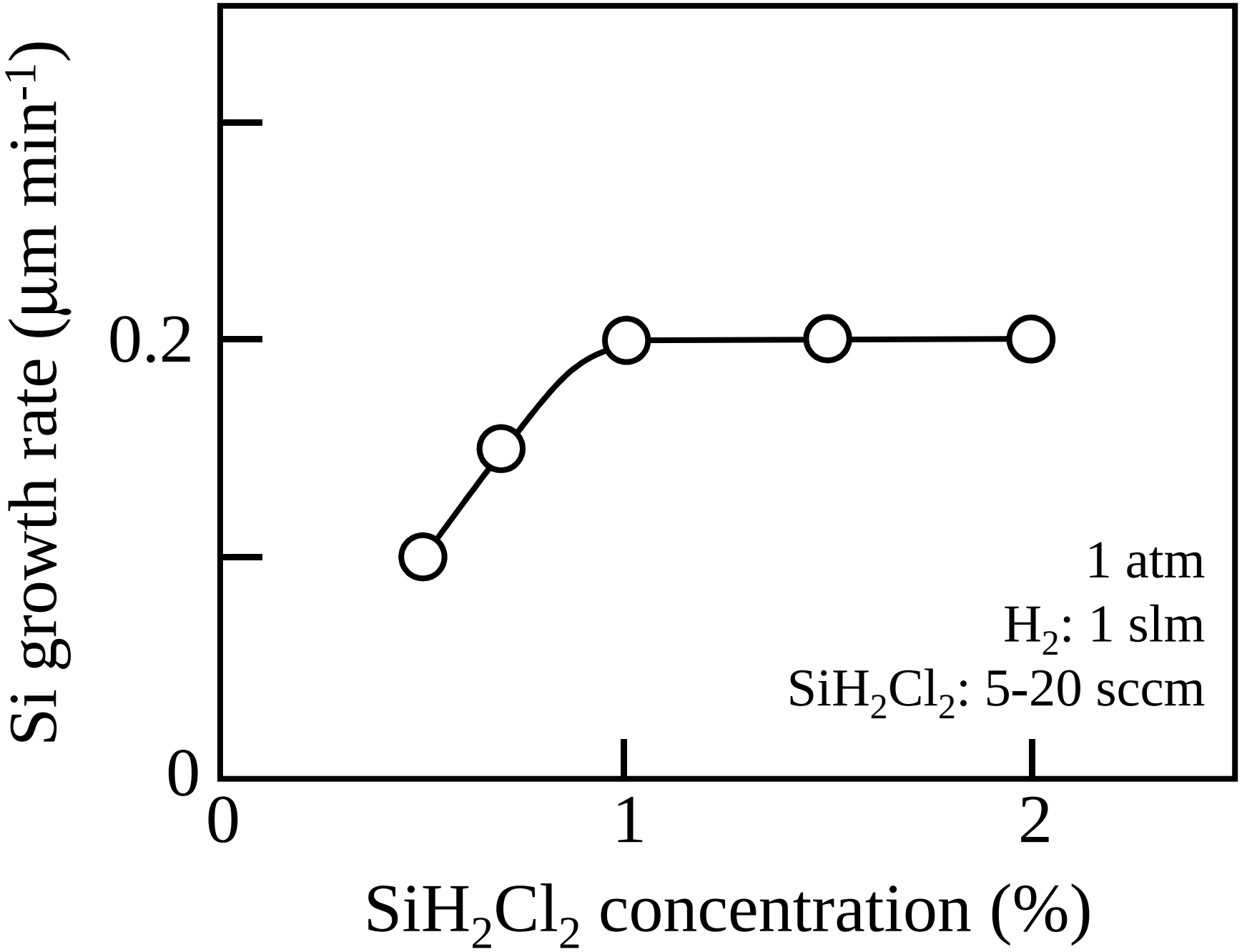
Si growth rate (μm min-1)
0.2
0
0
1
2
SiH2Cl2 concentration (%)
1 atm
H2: 1 slm
SiH2Cl2: 5-20 sccm

Fig. 3

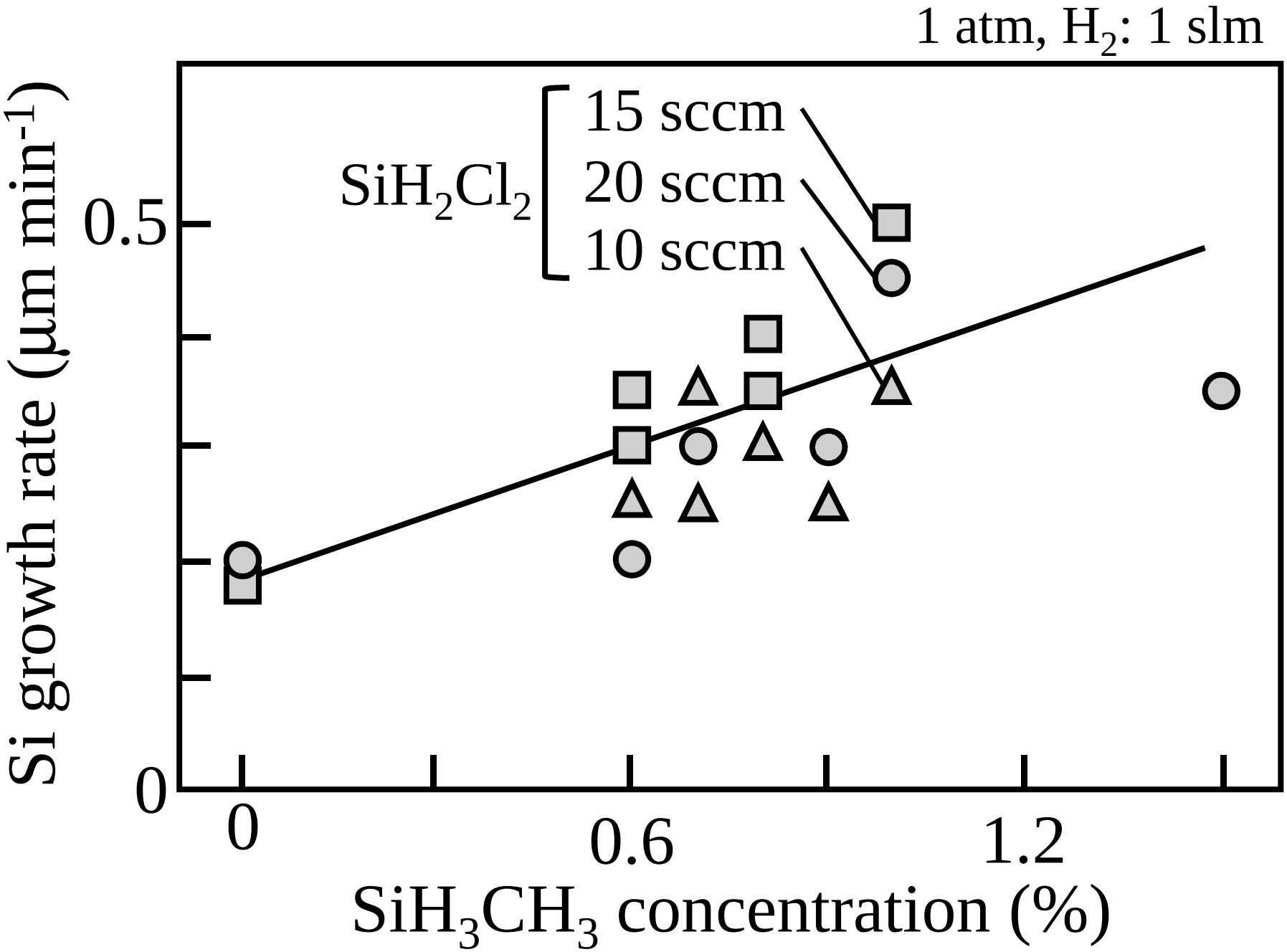
1 atm, H_2: 1 slm
SiH_2Cl_2
15 sccm
20 sccm
10 sccm
0.5
0
0
0.6
1.2
Si growth rate (μm min^{-1})
SiH_3CH_3 concentration (%)

Fig. 4

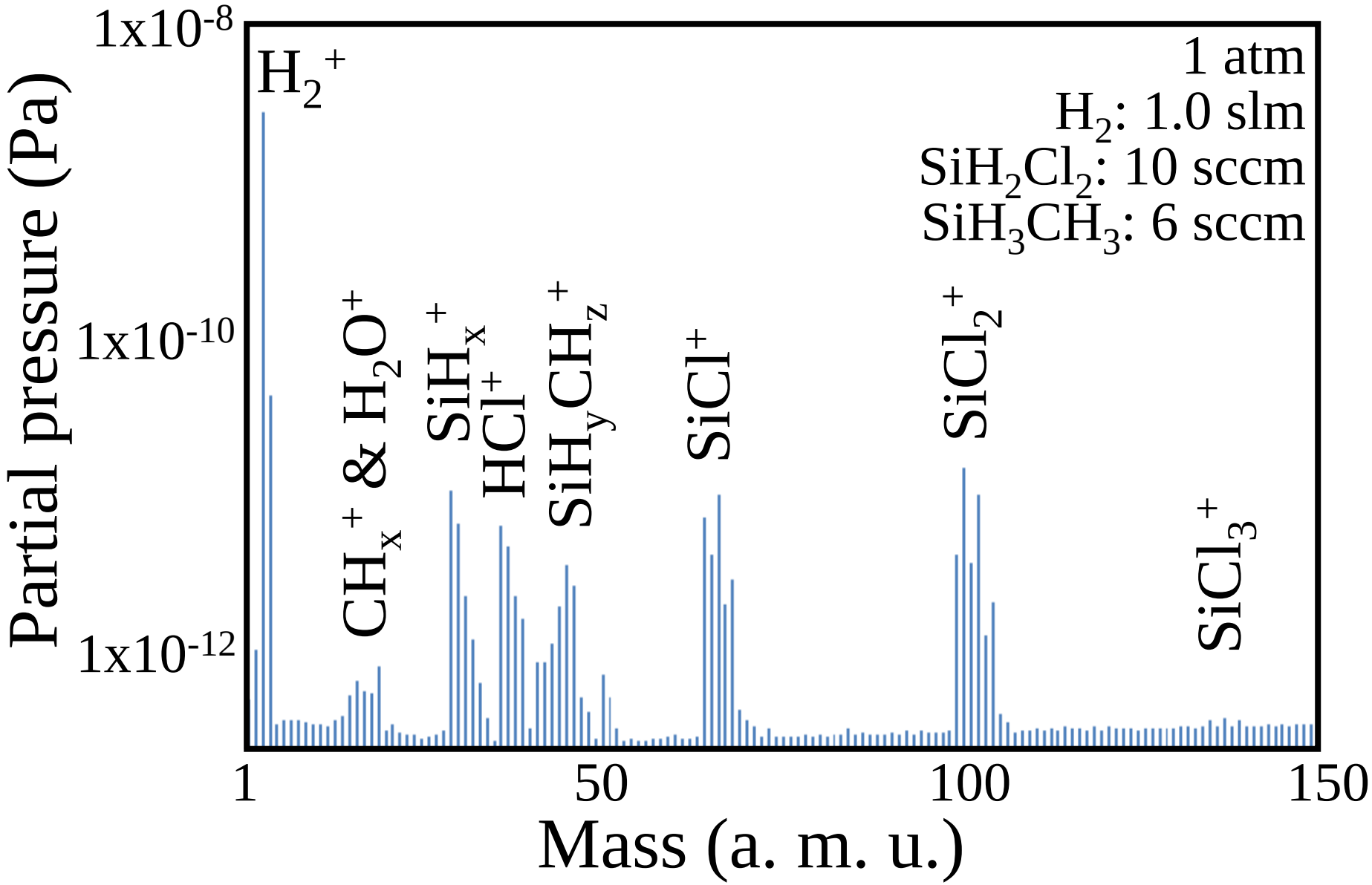
1x10-8
1x10-10
1x10-12
Partial pressure (Pa)
H2+
1 atm
H2: 1.0 slm
SiH2Cl2: 10 sccm
SiH3CH3: 6 sccm
CHx+ & H2O+
SiHx+
HCl+
SiHyCHz+
SiCl+
SiCl2+
SiCl3+
1
50
100
150
Mass (a. m. u.)

Fig. 5

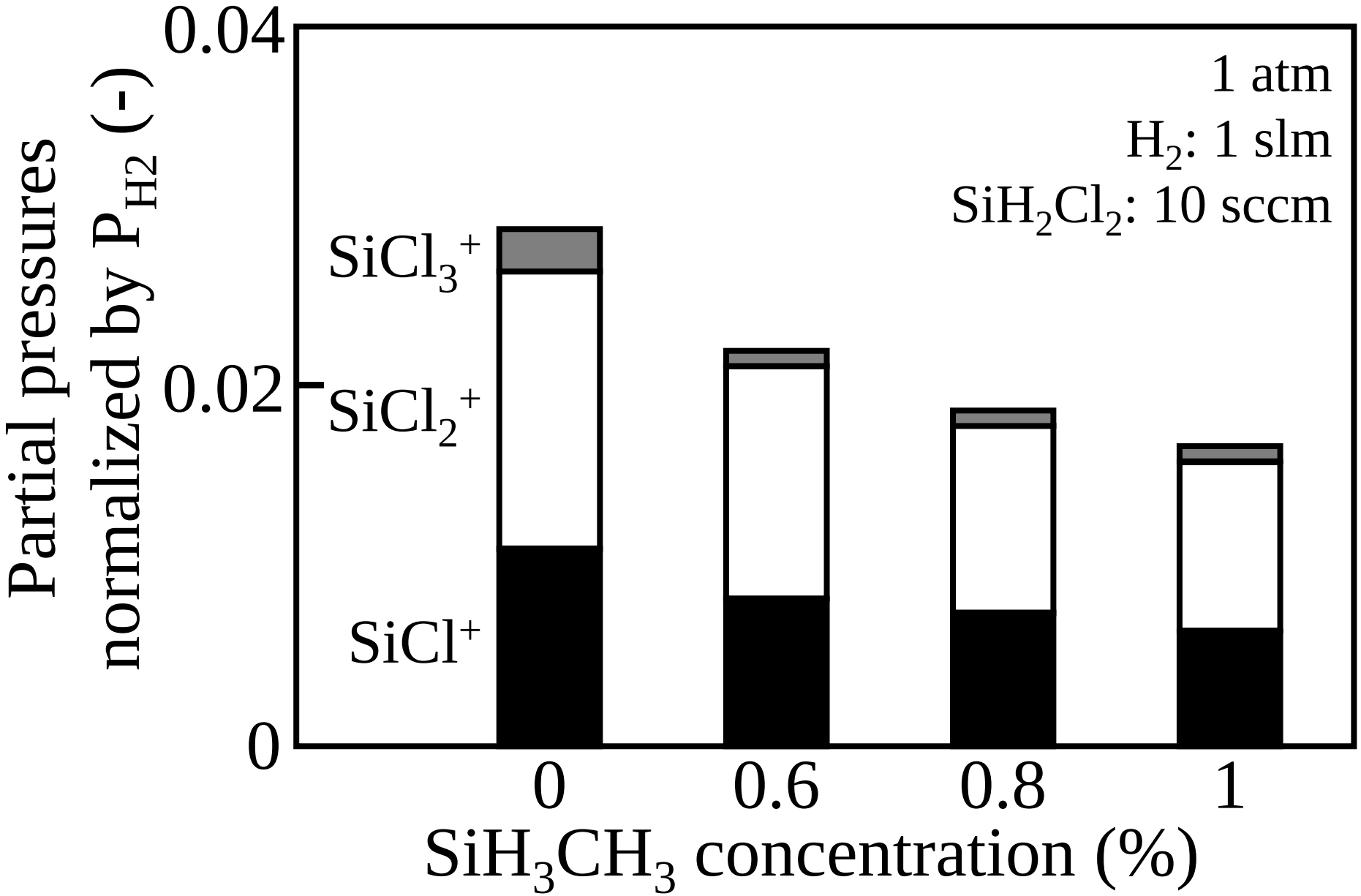
0.04
0.02
0
Partial pressures
normalized by P_{H2} (-)
1 atm
H_2: 1 slm
SiH_2Cl_2: 10 sccm
$SiCl_3^+$
$SiCl_2^+$
$SiCl^+$
0
0.6
0.8
1
SiH_3CH_3 concentration (%)

Fig. 6

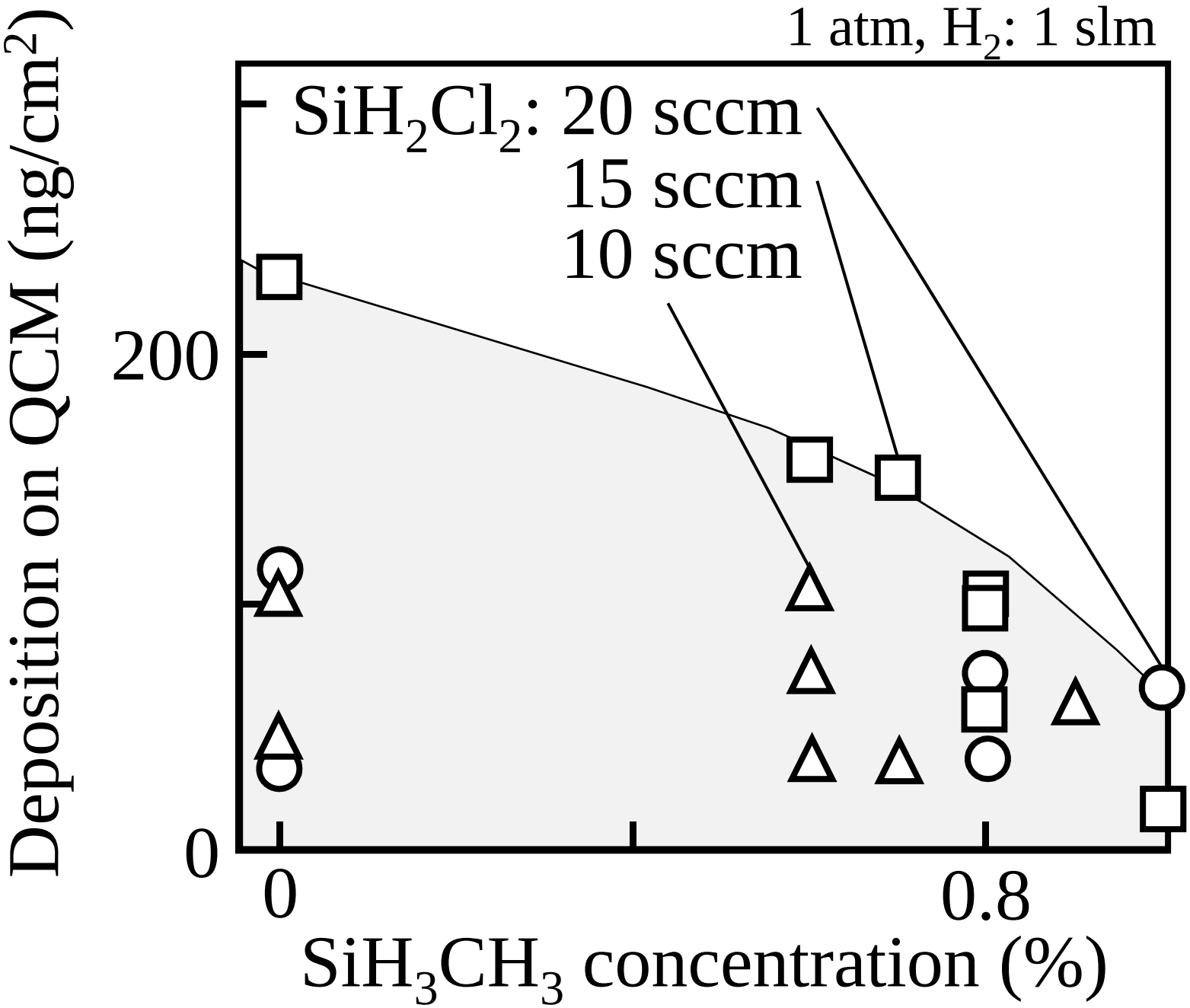
1 atm, H_2: 1 slm
SiH_2Cl_2: 20 sccm
15 sccm
10 sccm
200
0
0
0.8
Deposition on QCM (ng/cm^2)
SiH_3CH_3 concentration (%)

Fig. 7

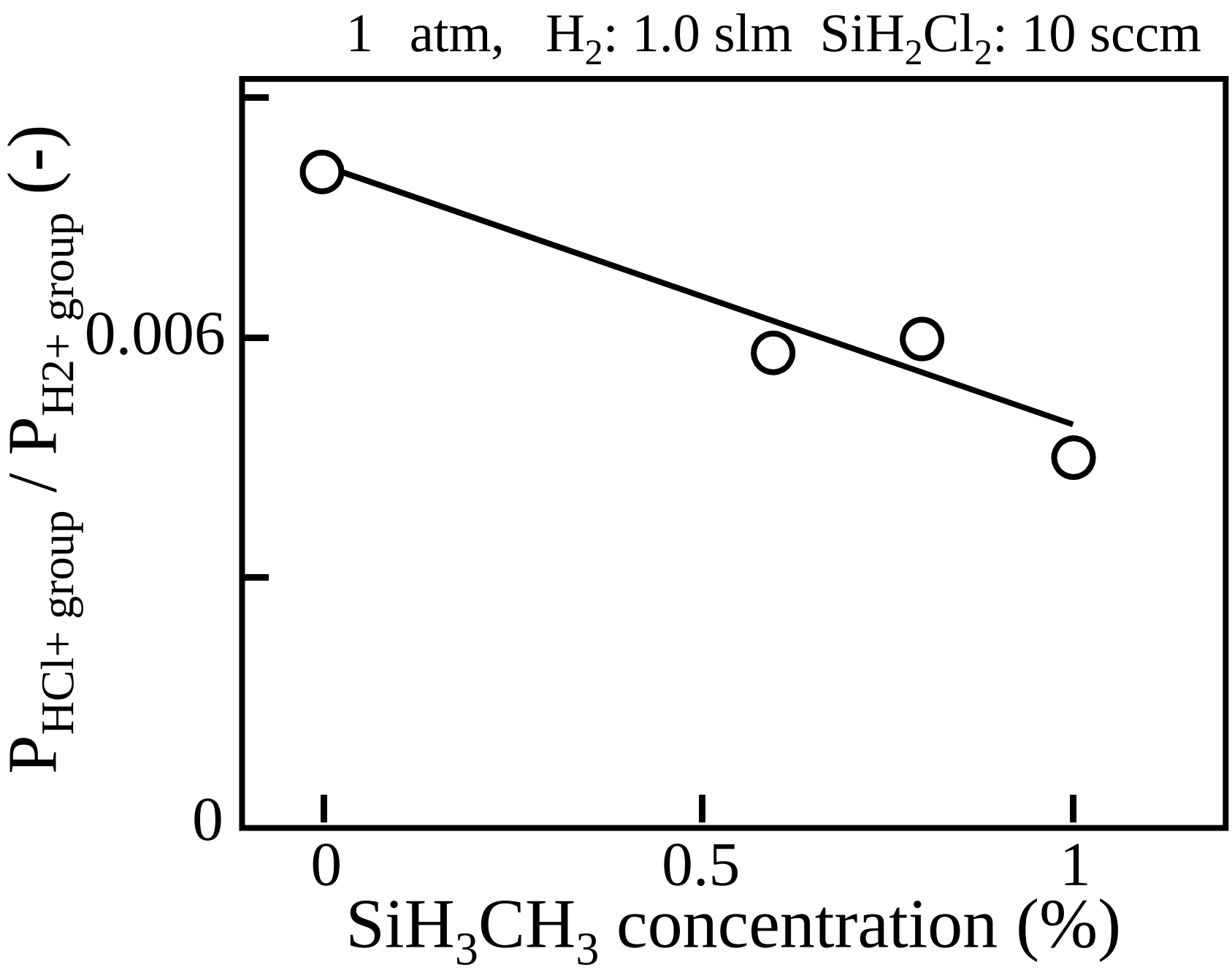
1 atm, H2: 1.0 slm SiH2Cl2: 10 sccm
P HCl+ group / P H2+ group (-)
0.006
0
0
0.5
1
SiH3CH3 concentration (%)

Fig. 8

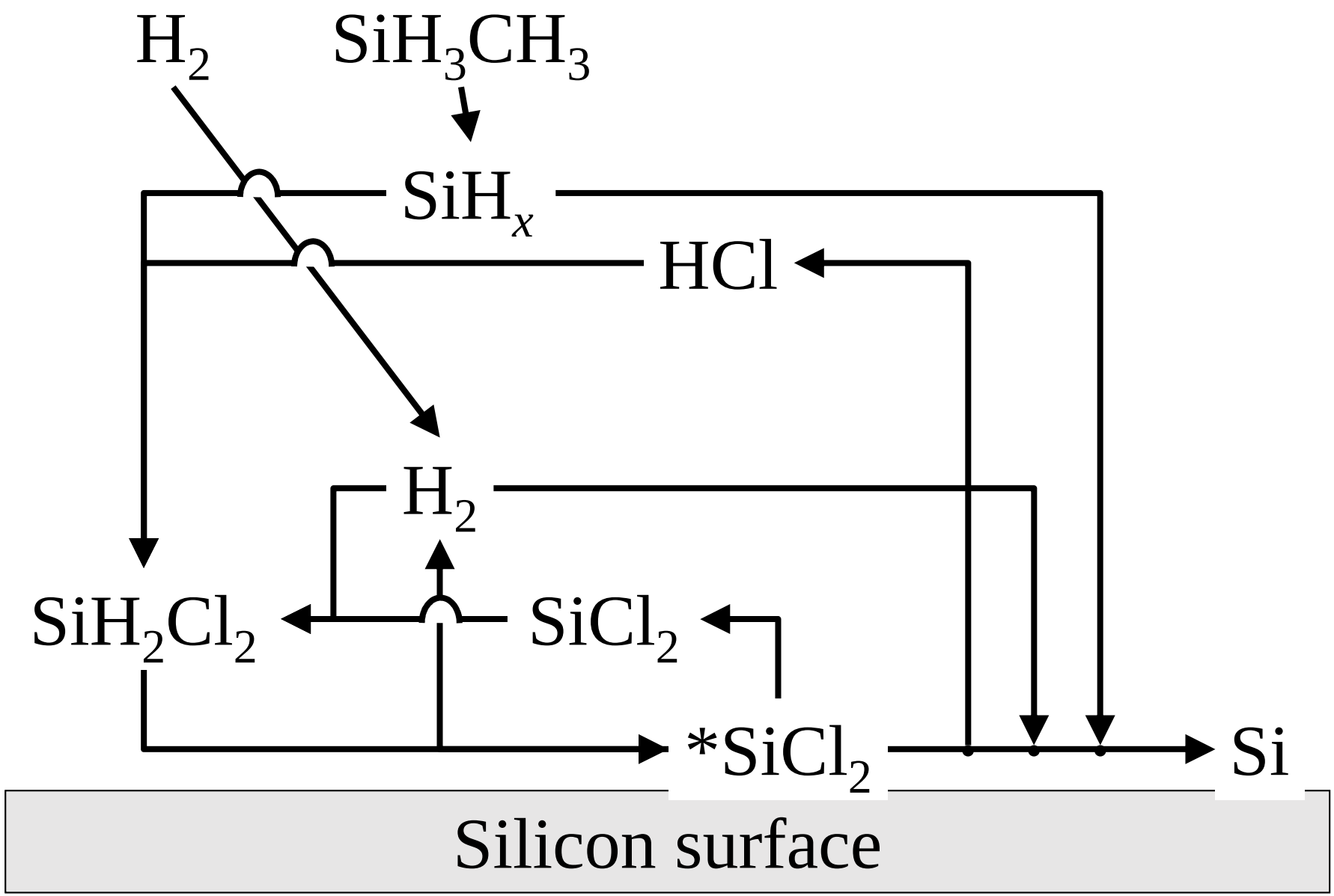
H2
SiH3CH3
SiHx
HCl
H2
SiH2Cl2
SiCl2
*SiCl2
Si
Silicon surface

Fig. 9